USING CENTRAL COMPOSITE EXPERIMENTAL DESIGN TO OPTIMIZE THE DEGRADATION OF REAL DYE WASTEWATER BY FENTON AND PHOTO-FENTON REACTIONS

Francesc Torrades[(1)]* and Julia García-Montaño[(2)]

(1) Departament d'Enginyeria Química, ETSEIA de Terrassa, Universitat Politècnica de Catalunya, C/Colom 11, E-08222, Terrassa (Barcelona) Spain.

(2) LEITAT Technological Center, Environment R&D Department, C/Innovació, 2, E-08225 Terrassa (Barcelona), Spain.

E-mail: francesc.torrades@upc.edu

FAX: 34937398101

TEL: 34937398148

Submitted to Dyes and Pigments

*To whom correspondence should be address

ABSTRACT

This work focuses in the use of Fenton reagent and UV-irradiation, in a lab-scale experiment, for the treatment of real dye wastewater coming from a Spanish textile manufacturer.

Response surface methodology (RSM) and a 2^3 factorial design were used to evaluate the effects of the three independent variables considered for the optimization of the oxidative process: temperature, Fe (II) and H_2O_2 concentrations, for a textile wastewater generated during a dyeing process with chemical oxygen demand (COD) of 1705 $mg \cdot L^{-1}$ O_2 at pH = 3. Wastewater degradation was followed in terms of COD decrease.

In the optimization, the correlation coefficients for the model (R^2) were 0.985 and 0.990 for Fenton and photo-Fenton treatments respectively. Optimum reaction conditions at pH = 3 and temperature = 298 K were $[H_2O_2]$ = 73.5 mM and [Fe(II)] = 1.79 mM.

The combination of Fenton, Fenton-like and photon-Fenton reactions has been proved to be highly effective for the treatment of such a type of wastewaters, and several advantages for the technique application arise from the study. Under these conditions, 120 min of treatment resulted in a 62.9 % and 76.3 % decrease in COD after Fenton and photo-Fenton treatments respectively.

Keywords: Advanced Oxidation Processes, Fenton, Photochemical reactions, real dye wastewater, central composite design

1. Introduction

Textile mills are major consumers of water with high average water consumption [1] and consequently one of largest groups of industries causing intense water pollution. Generated wastewaters collect different effluents from different manufacturing unitary operations: from raw material preparation processes (i.e., desizing, scouring and bleaching), as well as from dyeing, soaping, softening, etc. These complex operations, subjected to frequent changes as a result of shifting consumers preferences, are the cause of the variable volume and the wide diversity of chemical products found in these wastewaters. Though their characteristics depend on the specific operations performed, they commonly present suspended solids, high temperature, unstable pH, high chemical oxygen demand (COD), low biological demand (BOD) and high colourisation.

These effluents, produced in great quantities, contain appreciable levels of organic compounds which are not easily amenable to chemical or biological treatment [2,3] and can be very dangerous to environmental life [4]. Moreover, adsorbable organic halogens (AOX) are formed as a result of the use of bleaching chemicals [5].

Such wastewaters composition would cause serious impacts when encountering natural areas. High contents of organic matter originate depletion of dissolved oxygen, which has an adverse effect on the marine ecological system and the whole ecosystem [6].

As said before, a particularity of most of the textile effluents is their high levels of COD. In order to overvome this problem, a typical practice in textile and paper industry is the previous use of hydrolysis in basic media, in order to decrease initial COD levels. [7, 8].

In this frame, textile industry is confronted with the challenge of effective wastewater remediation.

A varied range of methods have been developed for textile wastewater treatment at laboratory, pilot or full scale. The most widely used are coagulation-floculation, foam flotation, membrane filtration, biological treatment and chemical processes [9-11]. However, most of these methods are quite inefficient or are not suitable when working with toxic and/or non biodegradable textile wastewaters [12]. Therefore, destructive treatment methods for the remediation of recalcitrant or hazardous pollutants are currently under investigation. In this direction and taking advantage of high oxidative power of the ·OH radical (2.8 V versus NHE), several advanced oxidation processes (AOPs) such photocatalysis, Fenton and photo-Fenton has been used in the remediation of textile wastewaters [13-15].

The effectiveness of these processes has a special interest and constant development [16]. Moreover, it makes possible the achievement of high reactions yields with a low cost treatment.

In Fenton's processes, the reactions related to generation of hydroxyl radicals and Fe^{2+} ion recovery, are the following:

$$Fe^{2+} + H_2O_2 \rightarrow Fe^{3+} + {}^{\bullet}OH + {}^{-}OH \qquad k = 76.5\ L\cdot mol^{-1}\cdot s^{-1} \qquad (1)$$

$$Fe^{3+} + H_2O_2 \leftrightarrow FeOOH_2^{+} + H^{+} \qquad K_{eq} = 3.10\cdot 10^{-3} \qquad (2)$$

$$FeOOH^{2+} \rightarrow HO^{\bullet}_2 + Fe^{2+} \qquad k = 2.70\cdot 10^{-3}\ s^{-1} \qquad (3)$$

$Fe^{3+} + HO^{\bullet}_2 \rightarrow Fe^{2+} + O_2 + H^+$ $\quad k < 2.00 \cdot 10^3 \ L \cdot mol^{-1} \cdot s^{-1}$

(4)

The rate of contaminants degradation can be considerably increased when ultraviolet light is simultaneously irradiated in the photo-Fenton's process [11]. Under irradiation, ferric ion complexes produce extra $HO^{\bullet}$ radicals and the recovery of Fe (II) which will further react with more H_2O_2 molecules in Fenton reaction (equation (1)):

$$Fe^{3+} + H_2O \rightarrow FeOH^{2+} + H^+ \quad (5)$$

$$FeOH^{2+} \xrightarrow{h\upsilon} Fe^{2+} + HO\cdot \quad \lambda \leq 410 \text{ nm} \quad (6)$$

Fenton processes depend on various variables, such as pH, temperature, source of light and the H_2O_2 and Fe^{2+} concentrations. The level of these variables is the key in the COD decrease and elimination of different organic compounds.

However, most of the literature studies on Fenton reagent treatment of textile wastewaters report decolourization efficiencies, but not COD removal or mineralization. Moreover, in these studies each variable was treated individually, while the other variables remain constant.

This high number of influential variables makes suitable using experimental design techniques. These techniques provide a systematic way of working that allows conclusions to be drawn about the variables or its combination, that are most influential in the response factors while carrying out the minimum possible number of experiments. Among these experimental designs, we can find the central composite

design (CCD), Doehlert matrices, Box-Behnken designs and three-level full-factorial designs [17].

We can find in literature some papers that use statistical design of experiments to develop optimal AOPs for wastewaters treatment. Several authors have studied the degradation of pulp and paper wastewaters [18,19] and textile wastewaters [20-22]. However, most of these papers are related to synthetic effluents. In consequence, the goal of the present work has been to identify, by using response surface methodology, optimum reaction conditions to degrade a real dye wastewater. As could be seen from obtained results, this wastewater could be successfully treated using Fenton and photo-Fenton reactions.

2. Experimental

2.1 Textile wastewater

The textile wastewater used in this study was collected from a textile industry located in Catalonia (North East of Spain). Particularly, this firm is dedicated to dyeing cotton fibres. This textile wastewater had a COD = 1705 $mg \cdot L^{-1}$ O_2, Total organic carbon (TOC) = 621 $mg \cdot L^{-1}$ C, supended solids (SS) = 33.18 $mg \cdot L^{-1}$, colour index = 1.412 cm^{-1} and pH = 7.4.

It was stored at 4 º C before use.

2.2. Chemicals

Iron sulphate ($FeSO_4 \cdot 7H_2O$, Merck 99,5 %) and hydrogen peroxide (H_2O_2 Panreac 33 % (w/v)) were used to obtain hydroxyl radical, $HO\cdot$.

Concentrated sulphuric acid and sodium hydroxide solutions were used to achieve desired pH values in working solutions.

Deionized water, from a Millipore Milli-Q system, was used to prepare all solutions.

2.2. Reactors and light sources

All Fenton's and photo-Fenton's experiments were carried out using a cylindrical Pyrex thermostatic cell of 150 ml of capacity. The reaction mixture consist in 100 ml of textile wastewater and necessary $FeSO_4 \cdot 7H_2O$ and H_2O_2. During all the treatment, solutions were stirred and temperature maintained at the required level [23].

As artificial source of light was used a 6 W Philips black light fluorescent lamp, which basically emits at 350-400 nm. The intensity of the incident UVA light, measured with a uranyl actinometer, was 1.38×10^{-9} Eienstein s^{-1}.

2.3. Analytical methods

Chemical Oxygen demand (COD, ($mg \cdot L^{-1}$ O_2)) was measured using the closed-reflux colorimetric method [24] with a HACH DR/2000 spectrophotometer.

Total Organic carbon (TOC, ($mg \cdot L^{-1}$ C)) was determined with a Shimadzu TOC-VCSH analyser with a solution of potassium phthalate as standard of calibration.

H_2O_2 consumption was measured using the KI titration method [25]. Remaining H_2O_2 was removed with sulphite [26]. Any remaining sulphite was removed by bubbling O_2.

3. Results and discussion

3.1. Operational conditions

The performance of Fenton's system depends of different variables like pH [11], initial Fe (II) and H_2O_2 dosage [27] and temperature [28]. Obviously a great number of experiments would be needed if all these variables were considered in the experimental design. If the role of these variables is previously known it will be possible to simplify the experimental analysis.

In this direction, it is known that the performance of such a complex reactive system is clearly pH dependent, particularly in Fenton-like and photo-Fenton reactions, with the maximum catalytic activity around pH =2.8 [29]. For higher pH values, low activity is detected because of decrease of free iron species due to ferric oxyhydroxides precipitation, formation of different complex species and break down of H_2O_2 to O_2 and H_2O. However, taking into account that different samples could exhibit optimal performance at different pH values, we tried Fenton's experiments at pH range between 2.0 and 4.0 and room temperature (298 K), in order to decide the best operating pH for our textile wastewater.

The treatment time was 120 min and the H_2O_2 and Fe (II) concentrations in these preliminary experiments were 2500 $mg \cdot L^{-1}$ (73.5 mM) and 100 $mg \cdot L^{-1}$ (1.79 mM), respectively. These doses are in accordance with stoichiometric requirements for COD

removal [23] and to prevent precipitation of ferric oxyhydroxides. The initial COD for textile wastewater was 1705 $mg \cdot L^{-1}$ O_2.

Fig. 1 shows that highest COD removal was obtained at a pH between 2.5 and 3.0. As said before, for higher pH values ferric oxyhydroxides precipitation occurs and free iron species decrease [30]. For pH's below 3 the activity decrease is due to the inhibition of complexation of Fe (III) with H_2O_2 and the photoactivity of Fe (II) species present in solution [31].

Consequently, the variable pH will be fixed at a value of 3 units.

3.2 Experimental design and statistical analysis

In this study, after the exploratory runs, to find the optimum conditions for degradation of textile wastewater under Fenton's and photo-Fenton's conditions, a central composite design (CCD) was applied, because of simple models (linear or quadratic) can be related to response factor (COD in our case). CCD is very commonly used form of response surface methodology (RSM) [32]. The second-order polynomial response equation was used to attain interaction between dependent and independent variables.

$$Y = b_0 + b_1X_1 + b_2X_2 + b_3X_3 + b_{12}X_1X_2 + b_{13}X_1X_3 + b_{23}X_2X_3 + b_{11}X_1^2 + b_{22}X_2^2 + b_{33}X_3^2 \quad (7)$$

where, Y is the % COD removal, X_i represents the three independent variables (Temperature, H_2O_2 and Fe (II) concentrations), and the b values represent regression coefficients.

A three level CCD consisting of 17 experiments was employed in this work. This method consisted in defining a low, central and high level, denoted as -1, 0 and +1 respectively (Table 1). Also, this design requires experiments outside the experimental range to allow the prediction of the response functions outside the cubic domain (denoted as ± 1.68; Table 1) [19]. The ranges of these values can be seen in Table 1 and were: T (K) = [298; 333]; (ii) H_2O_2 concentration (mM) = [55.1; 91.9]; and (iii) Fe(II) concentration (mM) = [0.895; 2.68].

The best operating range of temperature was chosen taken into account an expected increase in reaction efficiency with increasing temperature, the maximum temperature at what effluent was collected and accounting for the fact that higher temperatures can lead to H_2O_2 decomposition and loss of Fe (II) by precipitation [33]. H_2O_2 and Fe (II) range of operation were chosen taken into account stoichiometric requirements [34] and interference of too high iron and peroxide concentrations. These interferences could lead to a low efficiency of the process [35].

Table 2 presents results under dark Fenton and photo-Fenton conditions at pH = 3 and t = 120 min. treatment. Three of the experiments were conducted at the central points. For such replicates (runs 15-17), COD removal lies between 60.1 and 61.2 % in dark Fenton treatment and between 73.6 and 74.9 % in photo-Fenton treatment.

By using the Modde software (Umetrics), the following quadratic model for the experimental response was obtained:

Y_1 *(% COD removal, after 120 min. Fenton treatment)* = 60.70 (±3.75) -1.14 (±1.76)X_1 +2.63(±1.76)X_2 +8.87(±1.76)X_3 -2.48(±1.94)X_1^2 -7.25(±1.94)X_2^2 -13.49(±1.94)X_3^2 - 0.11(±2.30)$X_1 \cdot X_2$ +0.14(±2.30)$X_1 \cdot X_3$ +1.11(±2.30)$X_2 \cdot X_3$ (8)

Y_2 *(% COD removal, after 120 min. photo-Fenton treatment)* = 74.46 (±3.74) -1.10 (±1.75)X_1 + 3.27(±1.75)X_2 + 10.64(±1.75)X_3 -4.06(±1.93)X_1^2 -9.98(±1.93)X_2^2 -17.25 (±1.93)X_3^2 +0.09(±2.29)$X_1 \cdot X_2$ +0.14(±2.29)$X_1 \cdot X_3$ +1.89(±2.29)$X_2 \cdot X_3$ (9)

From equations (8) and (9) we predicted COD removal efficiencies. The obtained results are presented in Table 3. As it can be seen from these results, good agreements between experimental and predicted values for COD removal are obtained.

At this point, analysis of variance (ANOVA) was used to test the suitability of the model (Table 4). In the ANOVA test, the F-ratio value obtained for the percentage of COD removal is higher than the Fisher's F-value ($F_{9,7}$ = 3.80), and so one can conclude that the model fitted well. Moreover, the quality of the fit of the polynomial model was expressed by R^2 (correlation coefficient). From R^2 = 0.985 in Fenton treatment and R^2 = 0.990 in photo-Fenton treatment, we can say that 98.5 % and 99.0% of the response variability is explained by the model and the model does not explain only 1.5 and 1.0 % of variation respectively. From these values, we can state that a good correlation was obtained, indicating a good fit by the model, for which at least R^2 = 0.80 is suggested [36].

After checked model suitability, next point was the identification of significant variables and/or interactions, according to Student's *t*-test. It can be seen in Table 5 the obtained results. From these results, we can affirm that X_2 (H_2O_2) and X_3 (Fe (II)) concentrations have a positive effect on the response (P values smaller than 0.05 for 95 % confidence level) in both treatments. Also X_1^2 (T^2) had a slightly negative effect. However, X_1 (T) was negligible, in accordance with the fact that this variable is only important in the first stages of Fenton's reactions [28]. Fe (II) concentration has a stronger effect than H_2O_2 concentration.

Subsequently, a MODDE software to produce response surface plots was used. In figures 2 and 3, the response surface plots were presented as a function of H_2O_2 and Fe (II) concentrations; temperature was kept constant at 298 K and pH was maintained at 3 according to obtained results in section 3.1.

From figures 2 and 3, it can be concluded that the key parameter for the removal of COD, is the Fe(II) concentration. The effect of H_2O_2 is also important, but to a lower extent. H_2O_2 and Fe (II) concentrations affect positively the COD removal. However, when one moves towards higher Fe (II) or H_2O_2 concentrations, a detrimental effect in COD removal can be seen. The detrimental effect can be related with the scavenging of radicals, as it is shown in the following equations (10-12):

$$H_2O_2 + HO^{\cdot} \rightarrow HO^{\cdot}{}_2 + H_2O \quad (10)$$

$$Fe(II) + HO^{\cdot} \rightarrow Fe(III) + OH^{-} \quad (11)$$

$$Fe(II) + HO_2\cdot \rightarrow Fe(III) + HO_2^- \quad (12)$$

However, significant Fe(II) and H_2O_2 concentrations are needed to take place Fenton's reactions. The worst results are obtained at [Fe (II)] = 0.29 mM (the lowest level of Fe (II) used).

From these plots and the aforementioned comments, optimum conditions for the removal of COD were: pH =3; T = 298 K; [Fe(II)] = 1.79 mM and [H_2O_2] = 73.5 mM. Taking into account these conditions, an additional experiment was performed. As it can be seen in Fig. 4**,** a 62.9 % decrease in COD under Fenton treatment and 76.3% decrease under photo-Fenton treatment were obtained. This figure shows that in the first minutes of reaction no significant differences exist between both treatments, in terms of COD decrease. This fact can be explained by considering that the initial COD decrease is mainly due to dark Fenton reaction, which is faster than photo-Fenton reactions [37]. When increasing reaction times, important differences exist between the two treatments. UVA radiation improves COD removal. This fact is due to photolysis of ferric aquo-complexes producing extra HO· and the recovery of Fe (II) which will further react with more H_2O_2 molecules in Fenton reaction. Moreover, photoassisted process can also drive ligand-to-metal charge transfer in the potentially photolabile complexes formed by Fe (III) and organic compounds [29].

At this point a punctual TOC measure was performed after 62.9 % decrease in COD under Fenton treatment and 76.3% decrease under photo-Fenton treatment. We obtained a 58.1 and 70.4 % TOC reduction respectively. According to this, the remaining H_2O_2 is an important parameter that needs to be determined. Its value is needed in order to know

the reactions performance and when Fenton's reactions are employed connected to a biological treatment. As can be seen in Figure 5, where is represented remaining H_2O_2 vs. time, under optimal conditions for the dark Fenton and photo-Fenton reactions, a 2500 $mg \cdot L^{-1}$ H_2O_2 concentration (73.5 mM) is sufficient to degrade textile wastewater. The remaining H_2O_2 at the end of the treatments (120 min) is very low.

4. Conclusions

As can be seen from obtained results, textile wastewater can be successfully degraded under Fenton's and photo-Fenton conditions. This degradation depends on several variables. After preliminary runs, that demonstrated that pH should be maintained at three units, an empirical relationship between COD removal and independent variables was obtained. This relationship followed a second-order polynomial equation and the optimization procedure produced high and significant R^2 and R^2_{adj} values for both treatments, giving good accordance between the model and experimental data. These values were: 0.985 and 0.965 for Fenton treatment and 0.990 and 0.978 in the case of photo-Fenton treatment.

Among the studied variables, it can be seen that the largest effect in COD removal efficiency is due to Fe (II) concentration. Also, reaction could be carried out efficiently at room temperature.

In summary, the optimal reaction conditions to degrade this real dye wastewater were: pH =3; T = 298 K; [Fe (II)] = 1.79 mM and $[H_2O_2]$ = 73.5 mM. Under these conditions and with a 120-min treatment, it was possible to remove 62.9% and 76.3% COD in Fenton and photo-Fenton treatments, respectively. In addition, we can say that response

surface methodology (RSM) was an appropriate technique to optimize the operating conditions and maximize real dye wastewater removal.

Acknowledgement

The authors thank, Polytechnic University of Catalonia (Spain), for facilities and support in doing experimental work.

References

[1] EPA, Best management practices for pollution prevention in textile industry, manual 625R96004, Washington DC, USA 1996.

[2] Uygur A, Kök E. Decolorisation treatments of azo dyes wastewaters including dichlorotriazinyl reactive groups by using advanced oxidation method. J. Soc. Dyers Colour. 1999; 115: 350-54.

[3] Lin S.H and Peng, C.F., Treatment of textile wastewater by electrochemical method, Water Res. 1994; 28: 277-82.

[4] dos Santos A.B, Cervantes F.J, van Lier J.B, Review paper on current technologies for decolourisation of textile wastewaters: Perspectives for anaerobic biotechnology, Bioresour. Technol. 2007; 98: 2369-85.

[5] Delée W, O'Neil C, Hawkes F.R, Pinheiro H.M, Anaerobic treatment of textile effluents: a review. J. Chem. Technol. Biot. 1998; 73: 323-35.

[6] Kuo W.G, Decolorizing dye wastewater with Fenton's reagent. Water Res. 1992; 26: 881-86.

[7] Dorica J, Removal of AOX from bleach plant effluents by alkaline hydrolysis, J. Pulp Paper Sci. 1992; 18: 231-37.

[8] Torrades F, Peral J, Pérez M, Doménech X, García Hortal JA, Riva MC, Application of heterogeneous photocatalysis and ozone to destruction of organic contaminants in bleaching kraft mil effluents, Tappi J. 2001; 84 (6): 1-10.

[9] O'Neil C, Hawkes FR, Hawkes DI, Lourenço ND, Pinheiro HM, Delée W. Colour in textile effluents-sources, measurement, discharge consents and simulation: a review. J.Chem. Technol. Biotechnol. 1999; 74(11) 1009-18.

[10] Slokar YM, Majcen Le Marechal A. Methods for decolorization textile wastewatrers, Dyes Pigments 1998; 37: 335-6.

[11] Pignatello J, Oliveros E, MacKay A. Advanced oxidation processes for organic contaminant destruction based on the Fenton reaction and related chemistry. Crit. Rev. Environ. Sci. Technol. 2006; 36: 1-84.

[12] Lodha B, Chaudhari, S. Optimization of Fenton-biological treatment scheme for the treatment of aqueous dye solutions, J. Hazard. Mater. 2007; 148: 459-6.

[13] Lucas MS, Peres JA. Decolorization of the azo dye reactive Black 5 by Fenton and photo-Fenton oxidation. Dyes Pigments 2006; 71: 236-44.

[14] Alinsafi A, Evenou F, Adbulkarim EM et al., Treatmrnt of textile industry wastewater by supported photocatalysis, Dyes Pigments 2007; 74 (2): 439-445.

[15] Muruganandham M, Swaminathan M. Advanced oxidative decolourisation of Reactive Yellow 14 azo dye by UV/TiO_2, UV/H_2O_2, UV/H_2O_2/Fe^{2+} processes-a comparative study, Sep. Purif. Technol. 2006; 48: 297-03.

[16] Vilhunen S, Sillanpää M. Recent developments in photochemical and chemical AOPs in water treatment: a mini-review. Rev. Environ. Sci. Biotechnol. 2010; 9: 323-30.

[17] Ferreira SLC, Bruns RE, Ferreira HS, Matos GD. Box-Behnken design: an alternative for the optimization of analytical methods. Anal. Chim. Acta 2007; 597: 179-86.

[18] Pérez M, Torrades F, Peral J, Lizama C, Bravo C, Casas S, Freer J, Mansilla HD, Multivariate approach to photocatalytic degradation of a cellulose bleaching effluent, Appl. Catal. B: Environ. 2001; 33: 89-96.

[19] Torrades F, Saiz S, García-Hortal JA, Using central composite experimental design to optimize the degradation of black liquor by Fenton reagent, 2011; 268: 97-102.

[20] Arslan-Alaton I, Tureli G and Olmez-Hanci T. Optimization of the photo-Fenton-like process for real synthetic azo dye production wastewater treatment using response surface methodology. Photochem. Photobiol. Sci. 2009; 8: 628-38.

[21] Ay F, Cocay Catalkaya E, Kargi F. A statistical experiment design approach for advanced oxidation of Direct Red azo-dye by photo-Fenton treatment. J. Hazard. Mater. 2009; 162: 230-36.

[22] Rodrigues Carmen SD, Madeira LM, Boaventura Rui AR, Treatment of textile effluent by chemical (Fenton's Reagent) and biological (sequencing batch reactor) oxidation, J. Hazard. Mater. 2009; 172: 1551-59.

[23] Núñez L, García-Hortal JA, Torrades F, Study of kinetic parameters related to the decolourization and mineralization of reactive dyes fron textile dyeing using Fenton and photo-Fenton processes, Dyes Pigments 2007; 75: 647-52.

[24] APHA-AWWA-WPCF, Standard Methods for the Examination of Water and Wastewater. ASTM D1252-00, 17th ed., APHA-AWWA-WPCF, Washington, DC; 1989.

[25] Kormann C, Bahnemann DW, Hoffmann MR. Photocatalytic production of hydrogen peroxides and organic peroxides in aqueous suspensions of titanium dioxide, zinc oxide, and desert sand, Environ. Sci. Technol. 1988; 22: 798-06.

[26] Adams CD, Scanlan PA, Secrist ND, Oxidation and biodegradability enhancement of 1,4-dioxane using hydrogen peroxide and ozone, Environ. Sci. Technol. 1994; 28: 1812-18.

[27] Chamarro E, Marco A, Esplugas S, Use of fenton reagent to improve organic chemical biodegradability, Water Res. 2001; 35: 1047-51.

[28] Torrades F, García-Montaño J, García-Hortal JA, Núñez L, Domènech X and Peral J. Decolorisation and mineralisation of homo- and hetero-bireactive dyes under Fenton and photo-Fenton conditions. Color. Technol. 2004; 120: 188-94.

[29] Pignatello J, Liu D, Huston P, Evidence for an additional oxidant in the photoassisted Fenton reaction, Environ. Sci. Tecnol. 1999; 33: 1832-39.

[30] Oliveira R, Almeida MF, Santos L, Madeira LM. Experimental design of 2,4-dichlorophenol oxidation by Fenton's reaction. Ind. Eng. Chem. Res. 2006; 45: 1266-76.

[31] Safarzadeh-Amiri A, Bolton J.R and Cater SR, The use of iron in advanced oxidation processes, J.Advan. Oxid. Technol. 1996; 1: 18-26.

[32] Khtaee A.R, Zarei M, Asl SK. Photocatalytic treatment of a dye solution using immobilized TiO_2 nanoparticles combined with photoelectro-Fenton process: Optimization of operational parameters, J. Electroanal. Chem. 2010; 648: 143-50.

[33] Zapata A, Oller I, Bizani E, Sánchez-Pérez JA, Maldonado MI, Malato S. Evaluation of operational parameters involved in solar photo-Fenton degradation of a commercial pesticide mixture, Catal. Today 2009; 144: 94-9.

[34] Ince NH, Tezcanli G. Treatability of texyile dye-bath effluents by advanced oxidation: Preparation for reuse. Water Sci. Technol. 1999; 40: 183-90.

[35] Lin SH, Lo CC. Fenton process for treatment of desizing wastewater. Water Res. 1997; 31: 2050-056.

[36] Arslan-Alaton I, Tureli G and Olmez-Hanci T. Optimization of the photo-Fenton-like process for real synthetic azo dye production wastewater treatment using response surface methodology. Photochem. Photobiol. Sci. 2009; 8: 628-38.

[37] Pérez M, Torrades F, Domènech X, Peral J. Removal of organic contaminants in paper pulp effluents by AOPs: an economic study. J. Chem. Technol. Biotechnol. 2002; 77: 525-32.

Figure Legends

Fig. 1 Effect of initial pH on the COD removal from textile wastewater**,** for a treatment time of 120 min., $[H_2O_2]$ = 73.5 mM, [Fe(II)] = 1.79 mM and T=298 K.

Fig. 2 Response surface for the removal of COD from textile wastewater after 120 min. Fenton treatment, as a function of $[H_2O_2]$ and [Fe(II)] at T = 298 K and pH =3.

Fig. 3 Response surface for the removal of COD from textile wastewater after 120 min. photo-Fenton treatment, as a function of $[H_2O_2]$ and [Fe(II)] at T = 298 K and pH =3.

Fig. 4 Evolution of COD removal under optimal conditions (T = 298 K, pH =3, $[H_2O_2]$ = 73.5. mM and [Fe(II)] = 1.79 mM), for Fenton and photo-Fenton treatments.

Fig. 5 Residual H_2O_2 level as a function of time for textile wastewater, under optimal conditions for the dark Fenton and photo-Fenton reactions (T = 298 K, pH =3, initial $[H_2O_2]$ = 73.5 mM and [Fe(II)] = 1.79 mM).

Table 1

Levels of the parameters studied in CCD statistical experiment.

Variable	**Coded Variable**				
	-1.68	**-1**	**0**	**+1**	**+1.68**
T (K)	286	298	315.5	333	345
[H_2O_2]/(mM)	42.55	55.1	73.5	91.9	104.5
[Fe(II)]/(mM)	0.29	0.895	1.79	2.68	3.29

Table 2

Central Composite design matrix. Response factor results (%COD removal, after Fenton and photo-Fenton treatments).

				% removal	**% removal**
Run No.	T(K)	H_2O_2/(mM)	Fe (II)/(mM)	COD (Fenton)	COD (photo-Fenton)
1	-1 (298)	-1 (55.1)	-1 (0.895)	26.2	30.4
2	+1 (333)	-1 (55.1)	-1 (0.895)	26.4	30.6
3	-1 (298)	+1 (91.9)	-1 (0.895)	31.2	34.5
4	+1 (333)	+1 (91.9)	-1 (0.895)	30.9	34.8
5	-1 (298)	-1 (55.1)	+1 (2.68)	40.5	46.9
6	+1 (333)	-1 (55.1)	+1 (2.68)	41.2	47.4
7	-1 (298)	+1 (91.9)	+1 (2.68)	49.9	58.3
8	+1 (333)	+1 (91.9)	+1 (2.68)	50.2	59.4
9	-1.68 (286)	0 (73.5)	0 (1.79)	59.2	68.6
10	+1.68 (345)	0 (73.5)	0 (1.79)	49.4	58.4
11	0 (315.5)	-1.68 (42.55)	0 (1.79)	38.4	42.9
12	0 (315.5)	+1.68 (104.5)	0 (1.79)	43.2	50.6
13	0 (315.5)	0 (73.5)	-1.68 (0.29)	7.1	7.3
14	0 (315.5)	0 (73.5)	+1.68 (3.29)	39.2	45.1
15	0 (315.5)	0 (73.5)	0 (1.79)	60.6	74.9
16	0 (315.5)	0 (73.5)	0 (1.79)	61.2	73.6
17	0 (315.5)	0 (73.5)	0 (1.79)	60.1	74.7

Table 3

Predicted and experimentally achieved removal efficiencies for each run

% COD removal (Fenton)			**% COD removal (photo-Fenton)**		
Run No.	Actual	Predicted	Run No.	Actual	Predicted
1	26.2	28.3	1	30.4	32.5
2	26.4	25.9	2	30.6	29.8
3	31.2	31.5	3	34.5	35.1
4	30.9	28.8	4	34.8	32.8
5	40.5	43.5	5	46.9	49.7
6	41.2	41.7	6	47.4	47.6
7	49.9	51.2	7	58.3	59.8
8	50.2	49.0	8	59.4	58.1
9	59.2	55.6	9	68.6	64.8
10	49.4	51.8	10	58.4	61.1
11	38.4	35.8	11	42.9	40.7
12	43.2	44.6	12	50.6	51.7
13	7.1	7.6	13	7.3	7.8
14	39.2	37.5	14	45.1	43.6
15	60.6	60.7	15	74.9	74.5
16	61.2	60.7	16	73.6	74.5
17	60.1	60.7	17	74.7	74.5

Table 4

ANOVA results for % COD removal under Fenton and photo-Fenton treatments

	Source	df	SS	MS	F-ratio	P-value
Fenton	Model	9	3445.3	382.8	50.46	0.000
	Residual	7	53.11	7.59		
	Total	16	3498.4	218.65		
	$R^2 = 0.985$ $R^2_{adj.} = 0.965$					
Photo-Fenton	Model	9	5446.55	605.17	80.51	0.000
	Residual	7	52.62	7.52		
	Total	16	5499.2	343.7		
	$R^2 = 0.990$ $R^2_{adj.} = 0.978$					

Table 5

Estimates of the model regression for % COD removal under Fenton and photo-Fenton treatments

	Term	**Estimate**	**Standard error**	***t*-value**	**P-value**
Fenton	Intercept	60.7	1.59	38.2	0.000
	X_1	-1.14	0.745	-1.53	0.170
	X_2	2.63	0.745	3.53	0.009
	X_3	8.87	0.745	11.91	0.000
	X_1X_2	-0.11	0.97	-0.11	0.911
	X_1X_3	0.14	0.97	0.14	0.892
	X_2X_3	1.11	0.97	1.14	0.291
	X_1^2	-2.48	0.82	-3.02	0.019
	X_2^2	-7.25	0.82	-8.84	0.000
	X_3^2	-13.49	0.82	-16.45	0.000
Photo-Fenton	Intercept	74.5	1.58	47.2	0.000
	X_1	-1.10	0.74	-1.49	0.181
	X_2	3.27	0.74	4.42	0.003
	X_3	10.64	0.74	14.4	0.000
	X_1X_2	0.09	0.97	0.09	0.931
	X_1X_3	0.14	0.97	0.14	0.891
	X_2X_3	1.89	0.97	1.95	0.092
	X_1^2	-4.06	0.82	-4.95	0.002
	X_2^2	-9.98	0.82	-12.2	0.000
	X_3^2	-17.25	0.82	-21.0	0.000

Figure 1

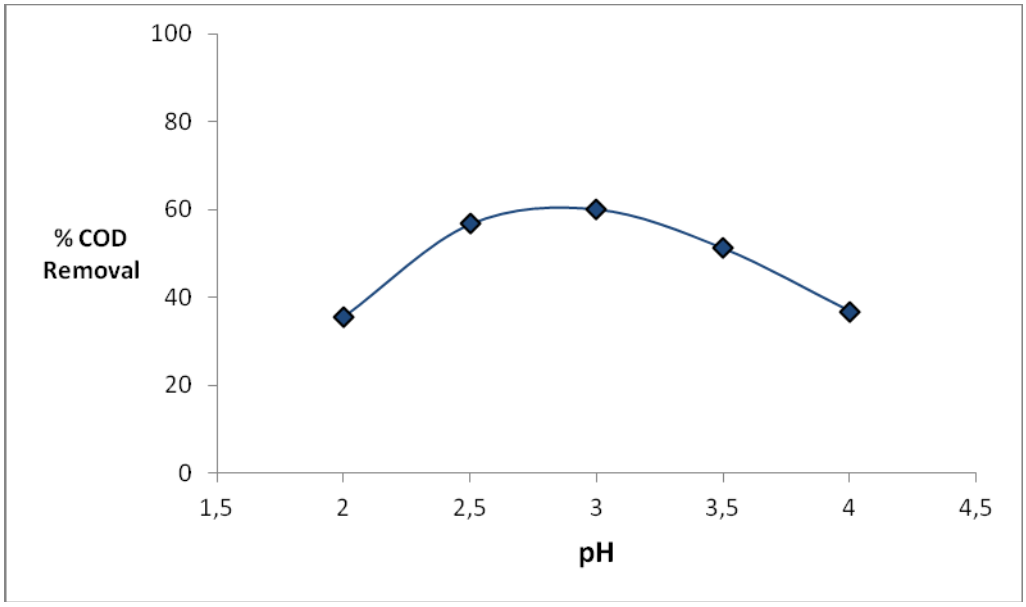

Figure 2

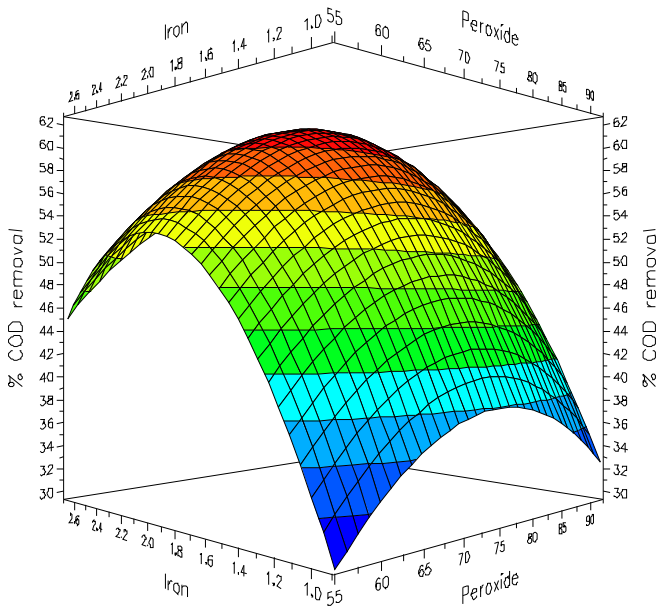

Figure 3

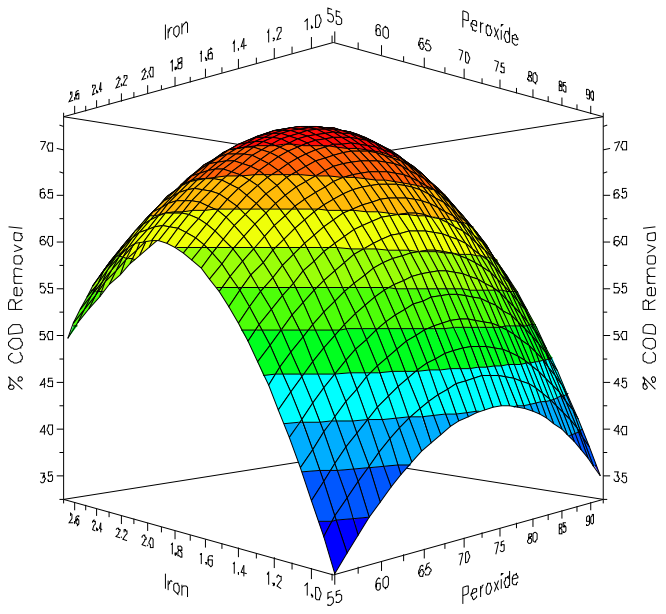

Figure 4

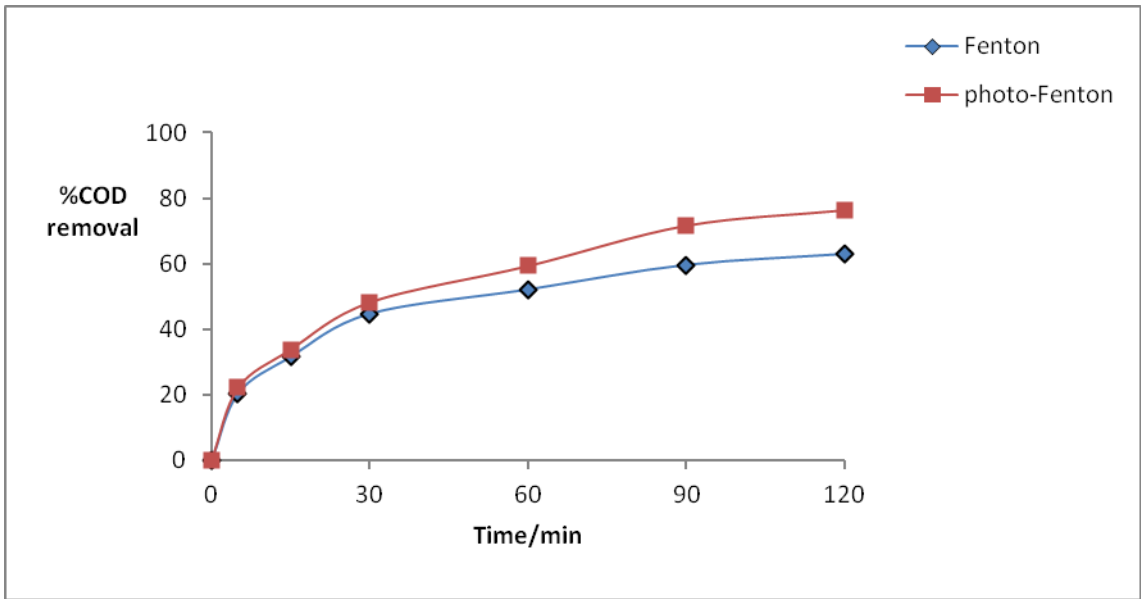
Fenton
photo-Fenton
%COD removal
100
80
60
40
20
0
0
30
60
90
120
Time/min

Figure 5

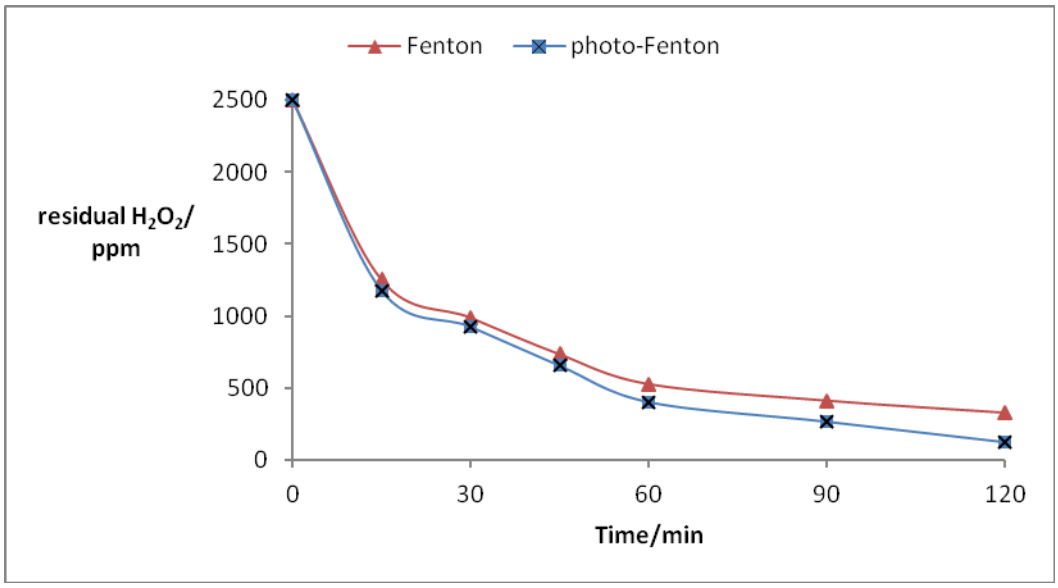
Fenton
photo-Fenton
residual H_2O_2/ ppm
2500
2000
1500
1000
500
0
0
30
60
90
120
Time/min